

Progress in theoretical understanding of properties of the heaviest nuclei

Adam Sobiczewski

Soltan Institute for Nuclear Studies, Hoza 69, PL-00-681 Warszawa, Poland

Fiz. Elem. Chastits At. Yadra **25**, 295–311 (March–April 1994)

A short review of recent theoretical results on the ground-state properties of the heaviest nuclei is given. Even–even nuclei with atomic number $Z=92$ –114 are considered. Much attention is paid to the role of shell effects in these properties.

1. INTRODUCTION

The objective of the present paper is to give a short review of theoretical results on the ground-state properties of the heaviest nuclei, obtained in recent years. Properties like deformation, mass, and alpha-decay and spontaneous-fission half-lives are discussed. To see some systematics of the properties, a rather large region of nuclei is considered. These are even–even nuclei with atomic number $Z=92$ –114.

Much attention is paid to the role of shell effects in the properties of these nuclei, which seem to have been underestimated in the past.

The reviewed theoretical studies are closely connected with extensive experimental research on the heaviest nuclei (cf., e.g., Refs. 1–7).

2. SPECIFIC FEATURES OF THE HEAVIEST NUCLEI

2.1. Instability

All nuclei of the considered region are unstable, i.e., radioactive. As we are interested in the nuclei which are not too far from the β -stability line, their main decay modes are alpha decay and spontaneous fission. Both modes are discussed in the present review.

2.2. Deformation

Most nuclei of the considered region are, or are expected to be, deformed. This is because their outer nucleons fill up large nuclear shells. For protons, this is the shell between the last experimentally known magic number $Z=82$ and the theoretically predicted number^{8,9} $Z=114$. Thus, the shell is as large (32 protons) as the largest experimentally observed proton shell between $Z=50$ and 82. For neutrons, this is the shell between the last experimentally known magic number $N=126$ and the theoretically predicted number^{8,9} $N=184$. If the predictions are correct, this shell would be the largest neutron shell (58 neutrons) of all those considered up to now. The largest experimentally observed shell is between the magic numbers $N=82$ and 126 (i.e., 44 neutrons).

2.3. Essential role of shell effects

Shell effects are important for all nuclei. Their role for the heaviest nuclei is, however, essential, as many of them would not exist at all without these effects. This will be discussed in more detail in the next section.

3. SHELL EFFECTS

Figure 1, taken from Ref. 10, illustrates shell effects in the masses of the heaviest nuclei, $M^{\text{exp}} - \tilde{M}$. Here, M^{exp} is the experimental mass and \tilde{M} is the mass calculated by the macroscopic model without any shell effects. For the latter, the widely used Yukawa-plus-exponential model¹¹ is taken. One can see that the shell effect is negative, i.e., it decreases the masses of the nuclei. Its absolute value increases with increasing atomic number Z , up to about 5 MeV for the heaviest known even–even nuclei $^{260}_{106}\text{U}$ and $^{264}_{108}\text{U}$.

Figure 2 (Ref. 10) shows the logarithm of the spontaneous-fission half-lives: experimental and calculated values within a macroscopic model without any shell effects. Thus, the difference between the two is the shell effect in the spontaneous-fission lifetime. Instead of showing this difference directly, we show here the half-life itself, to see its values; in particular, to see how fast the half-life T_{sf} decreases with increasing atomic number Z . For example, the value calculated for the nucleus $^{260}_{106}\text{U}$ with $Z=106$ is about 40 orders of magnitude smaller than the values obtained for nuclei with $Z=92$ (U).

The macroscopic calculation of T_{sf} performed here consists in using the Yukawa-plus-exponential model (Y) (Ref. 11) for the calculation of the fission barrier, and a smooth phenomenological model^{12–14} for the calculation of the mass (inertia) parameter, which describes the inertia of a nucleus with respect to changes of its deformation.

One can see in Fig. 2 that the shell effect delays the fission process in all the considered nuclei, except in only a few of the lightest ones (isotopes of uranium). The delay increases from a few orders (Pu isotopes) to about 15 orders of magnitude for the heaviest even–even nucleus with measured T_{sf} ($^{260}_{106}\text{U}$). For a heavy nucleus like $^{260}_{106}\text{U}$, with T_{sf} of the order of few milliseconds, this increase makes up practically the whole half-life of these nuclei. In other words, they would not exist without shell effects.

The mechanism by which practically the whole half-life of a very heavy nucleus is made up by shell effects is illustrated in Fig. 3. The illustration is given¹⁰ for the heaviest even–even nucleus observed up to now, i.e., for $^{264}_{108}\text{U}$. Here, the total fission barrier ($Y + \text{SHELL}$), including shell effects, is shown by the solid line, and its smooth part [obtained by the Yukawa-plus-exponential model (Y)] by the dashed line. The smooth barrier obtained by another macroscopic model (liquid drop,¹⁵ LD) is also shown (dotted line) for comparison. One can see

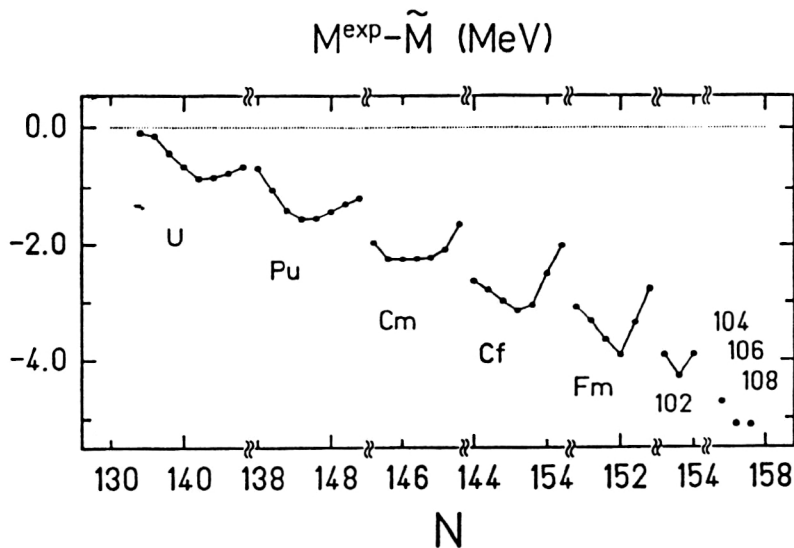


FIG. 1. Shell effects in the masses of nuclei.¹⁰

that a significant height (about 6 MeV) of the fission barrier is obtained only after the inclusion of shell effects. Without them, no fission barrier (Y and LD) appears.

Figures 1 and 2 illustrate the strong dependence of shell effects on the proton, Z , and neutron, N , numbers. This means that each nucleus should be treated individually (i.e., without any averaging over a number of nuclei) in a theoretical analysis. The strong dependence of shell effects also on the deformation of a nucleus, illustrated in Fig. 3, requires a careful treatment of this deformation in the analysis. In other words, the analysis of the properties of a heavy nucleus should be performed in a sufficiently large, multidimensional deformation space.

4. BIMODAL FISSION

It is known that nuclei around heavy isotopes of fermium show some peculiarities in their spontaneous-fission

properties. One of them is a rapid decrease of the asymmetry in the mass distribution of the fission fragments with increasing neutron number N (e.g., Ref. 16). Another peculiarity is that the average total kinetic energy, TKE, of the fission fragments does not follow the smooth systematics when one is approaching the heaviest isotopes of these nuclei.¹⁶ For example, for ^{258}Fm (and also ^{259}Fm), TKE is much larger than expected from this systematics. A careful analysis of the distribution of the total kinetic energy, TKE, performed^{17,18,5} for ^{258}Fm and few other nuclei close to it resulted in the separation of two components. One of them has a peak at TKE of about 200 MeV and corresponds to the "normal" mode of fission, which follows the above-mentioned systematics of TKE. The other has a peak at TKE of about 235 MeV and, thus, corresponds to a new mode with a higher kinetic energy of the fragments. The appearance of two different modes in the fission of the

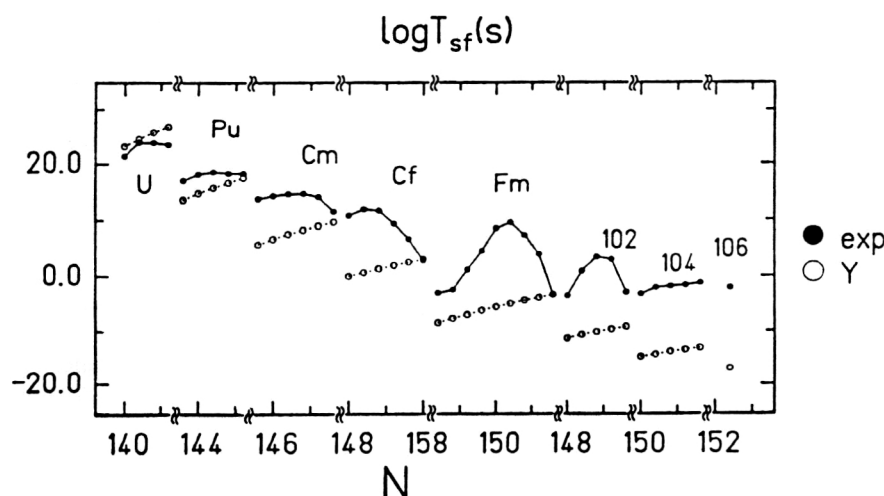


FIG. 2. Logarithms of the experimental (exp) and macroscopic (Y) spontaneous-fission half-lives T_{sf} (in sec).¹⁰

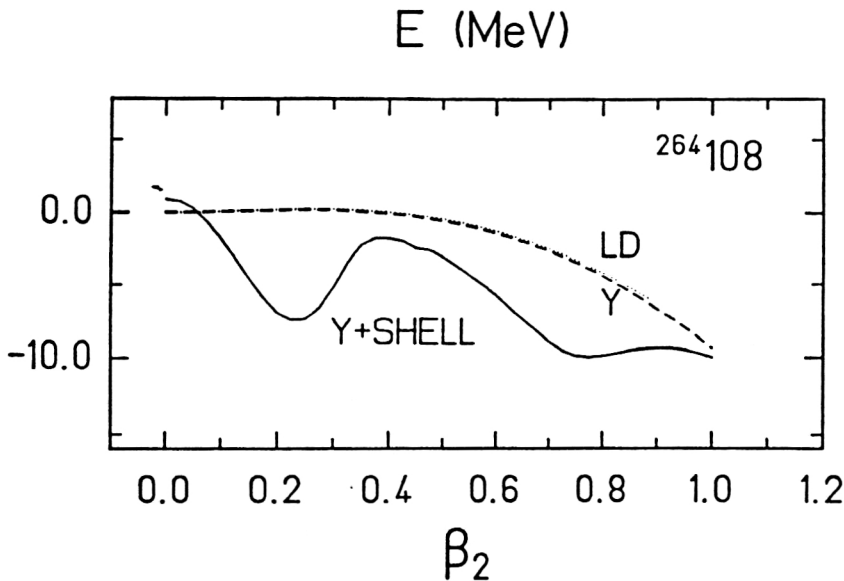


FIG. 3. Total fission barrier ($Y + \text{SHELL}$) and its smooth part obtained by the Yukawa-plus-exponential (Y) and liquid-drop (LD) models, for the nucleus $^{264}_{108}$ (Ref. 10).

same nuclide (i.e., in the fission of nuclei with the same Z and N) has been called “bimodal fission.”¹⁷

As TKE comes from the Coulomb repulsion energy between the fragments in the scission configuration, the low-energy component should correspond to more elongated shapes (ES), and the high-energy component to more compact shapes (CS), at the scission point. Thus, the simultaneous appearance of both modes of fission for some nuclei means that there should exist two different trajectories for each of these nuclei: one ending at the ES scission point and the other at the CS point, but both corresponding to the same fission barrier (to have the same fission half-life).

It was natural then to look at the potential energy, calculated theoretically, to see whether it predicts such trajectories. A number of calculations have been undertaken (e.g., Ref. 19–23). Some of the results will be illustrated in Sec. 6.

5. METHODS OF THEORETICAL DESCRIPTION

As mentioned in the Introduction, the main properties of the heaviest nuclei, in which we are interested in the present paper, are the alpha-decay and spontaneous-fission half-lives, T_α and T_{sf} respectively. To describe T_α , one needs to know the energy (mass) of the initial (parent) and final (daughter) nuclei. For the description of T_{sf} , the dependence of the energy of a nucleus on its deformation (fission barrier) as well as its inertia (mass parameters) are needed.

5.1. Energy of a nucleus

The energy of a nucleus is usually calculated by the macroscopic–microscopic method. The Yukawa-plus-exponential model¹¹ or the liquid-drop model¹⁵ is used for the macroscopic part of the energy. The Strutinsky shell

correction²⁴ is generally taken for the microscopic part. It is based on a single-particle potential, describing the internal structure of a nucleus. This is usually the Nilsson,²⁵ Woods–Saxon,²⁶ or folded-Yukawa²⁷ potential. The residual pairing interaction is usually treated in the BCS approximation (e.g., Ref. 28).

5.2. Inertia tensor

The inertia tensor provides the metric in a multidimensional deformation space and is necessary to find the fission trajectory. It is usually calculated in the cranking approximation (e.g., Refs. 14 and 29–32).

5.3. Parametrization of the deformation

There are a number of parametrizations of nuclear shapes. In most of the results presented in the present paper, the shapes are described by the usual deformation parameters β_λ appearing in the expression for the nuclear radius (in the intrinsic frame of reference) in terms of spherical harmonics,

$$R(\vartheta) = R_0(\beta_\mu) \left[1 + \sum_{\lambda=2}^{\lambda_{\max}} \beta_\lambda Y_{\lambda 0}(\vartheta) \right],$$

where the dependence of R_0 on β_μ is determined by the volume-conservation condition.

The shapes described by this formula are axially symmetric. More general shapes include a nonaxiality in the quadrupole ($\lambda=2$) (Refs. 33 and 34) and hexadecapole ($\lambda=4$) (Refs. 35–38) components of the deformation.

5.4. Alpha-decay half-lives

Alpha decay is usually described by a simple one-body model of this process. The alpha particle is assumed to be

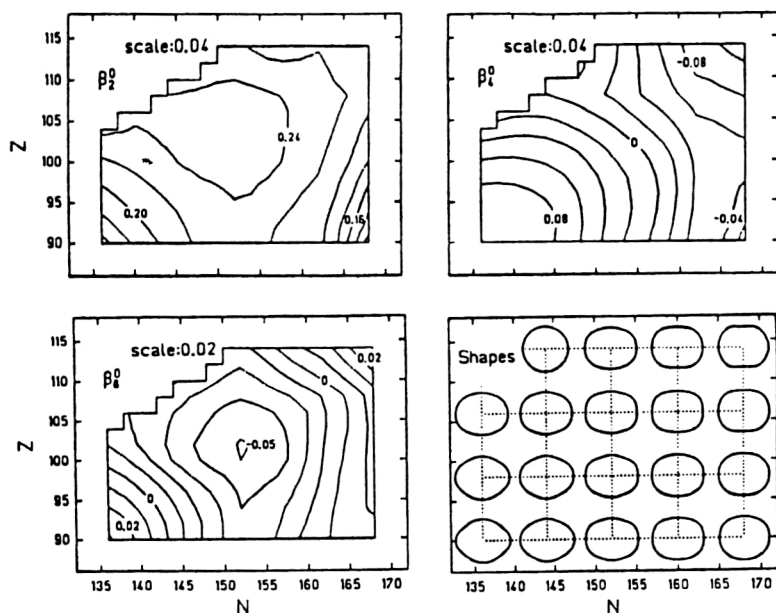


FIG. 4. Equilibrium deformations β_λ^0 ($\lambda = 2, 4, 6$) and shapes of nuclei. The numbers at the contour lines give the values of the deformation. They are obtained by minimization of the energy in the $\beta_2, \beta_4, \beta_6$ degrees of freedom. The difference in the values between neighboring solid lines is specified by the scale. The dashed lines divide this difference by two.⁴⁶

already formed in the parent nucleus, before its emission, and the decay consists in the penetration of this particle through the potential-energy barrier. The model leads to a simple expression for the half-life T_α in terms of the decay energy Q_α (e.g., Refs. 39–42). One of the forms of this expression is the phenomenological formula of Viola and Seaborg:³⁹

$$\log T_\alpha = (aZ + b)Q_\alpha^{-1/2} + (cZ + d),$$

where Z is the atomic number of the parent nucleus, Q_α is the alpha-decay energy in MeV, T_α is given in sec, and a, b, c, d are adjustable parameters. These parameters have been readjusted in Ref. 43 to take into account new data. Their values are

$$a = 1.66175, \quad b = -8.5166, \quad c = -0.20228,$$

$$d = -33.9069.$$

These new values allow one to reproduce the data better (especially for the heaviest nuclei) than the old values of the original paper,³⁹ by up to about one order of magnitude.

5.5. Spontaneous-fission half-lives

The spontaneous-fission half-lives T_{sf} have usually been calculated in two ways: by the static method (e.g., Refs. 13 and 21) and by the dynamical method (e.g., Refs. 30, 31, 44, and 45).

In the static method, the action integral (which determines the probability of penetration of a nucleus through the fission barrier) is calculated along the static trajectory, at every point of which the potential energy is minimal.

The inertia of a nucleus is taken in a phenomenological form,^{12–14} which seems, however, to be too simple. In particular, it does not take into account the shell structure of a nucleus, which is so important for the heaviest nuclei. In the dynamical approach, the half-life T_{sf} is calculated along the dynamical trajectory which minimizes the action integral (the integral is usually not minimal along the static trajectory). The trajectory is determined then by both the potential energy and the inertia tensor of a nucleus. The inertia tensor is usually calculated by the cranking method (as already mentioned above), which takes into account the microscopic (shell) structure of a nucleus.

In the present paper, we will illustrate the results for T_{sf} obtained in the dynamical calculations.

6. SOME THEORETICAL RESULTS

6.1. Ground-state deformations

Figure 4 (Ref. 46) gives the equilibrium deformations β_λ^0 ($\lambda = 2, 4, 6$) and the shapes of nuclei with proton number $Z = 90–114$ and neutron number $N = 136–168$. One can see that all nuclei in the studied region are deformed. The quadrupole deformation β_2^0 is rather large and does not vary much, especially around the center of the region. The hexadecapole deformation β_4^0 decreases from about $\beta_4^0 \approx 0.10$, for the lightest considered nuclei, down to about $\beta_4^0 \approx -0.09$, for the heaviest nuclei. The fastest variations are obtained for β_6^0 , which changes sign twice inside the considered region.

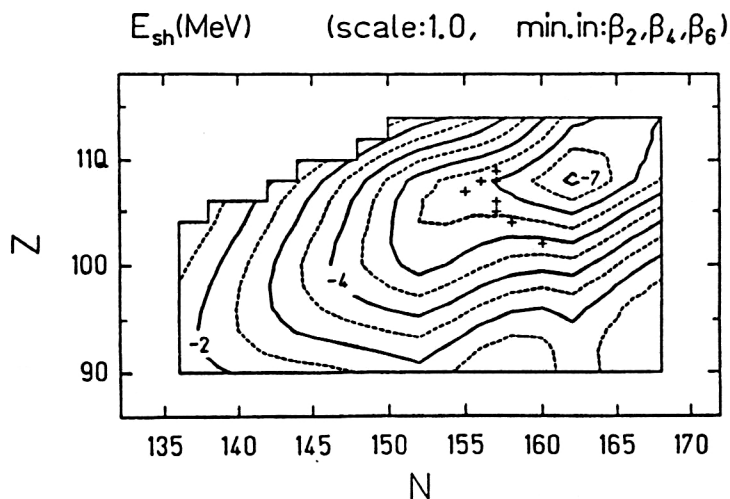


FIG. 5. Shell correction, E_{sh} to the potential energies of nuclei.⁴⁶

6.2. Shell correction to the energy

Figure 5 shows a map⁴⁶ of the shell correction, E_{sh} , to the potential energy. This correction is the gain in the potential energy of a nucleus due to its shell structure. One can see that the correction is negative in the whole region, i.e., it increases the binding of the nuclei. Starting from about 2 MeV (in absolute value), it systematically increases, up to about 7 MeV, as one passes from the beginning of the region to about its end. The large value of E_{sh} obtained for nuclei around $^{270}_{108}$ is associated with the new deformed shell at neutron number $N=162$. The experimentally known deformed shell at $N=152$ manifests itself here by a shallow local minimum in the E_{sh} map. Crosses in the figure indicate the heaviest nuclei synthesized up to now. One can see that these nuclei gain about

5–6 MeV in energy from the shell correction. Without this gain they could not exist, as was illustrated in Fig. 3.

Figure 6 gives a comparison⁴⁶ of the experimental (shown earlier in Fig. 1) and theoretical shell corrections to the mass of a nucleus. One can see that, except for the lightest isotopes of uranium, the experimental values are rather well reproduced by the calculations. In particular, the effect of the deformed neutron shell at $N=152$ is well reproduced in all elements ($Z=96-102$) for which it is observed experimentally. It is worth mentioning that the inclusion of the deformation β_6 in the analysis is important for this reproduction.

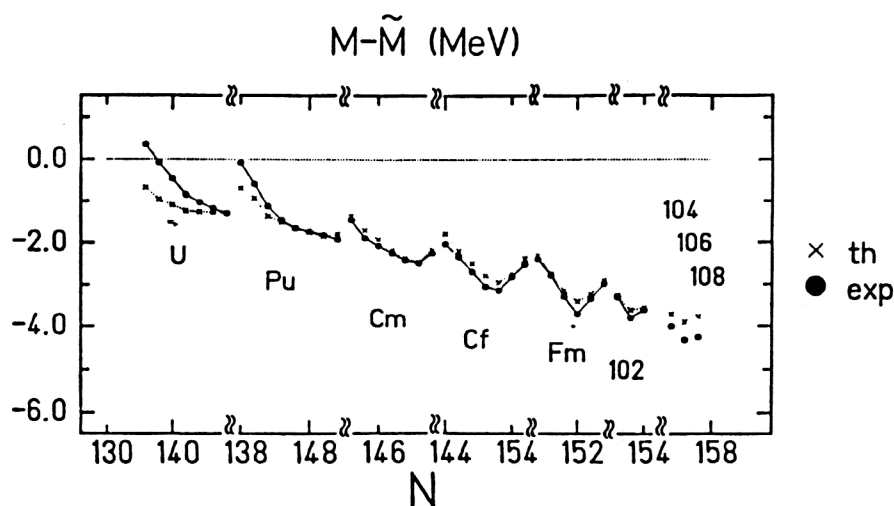


FIG. 6. Comparison of the theoretical (th) and experimental (exp) shell corrections to the mass of a nucleus, $M-\tilde{M}$ (Ref. 46).

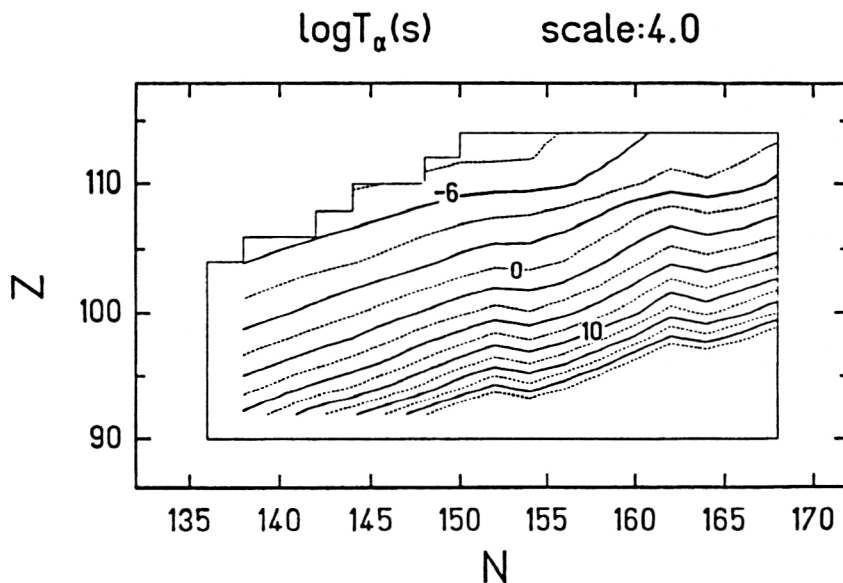


FIG. 7. Contour map of the logarithm of the alpha-decay half-life T_α , given in sec.⁴⁶

6.3. Alpha-decay half-lives

A map⁴⁶ of the logarithm of the alpha-decay half-life T_α is shown in Fig. 7. The half-life is calculated by the Viola-Seaborg phenomenological formula.³⁹ The parameters of the formula have been taken, however, from Ref. 43, where they were readjusted to take into account new data. A rather smooth behavior of T_α is seen. It decreases rapidly with increasing Z . The effect of closed deformed shells at neutron numbers $N=152$ and 162 is visible in the form of local maxima of T_α at these numbers.

6.4. Spontaneous-fission half-lives

Figure 8 shows a contour map⁴⁵ of the logarithm of the spontaneous-fission half-life T_{sf} , calculated dynamically for even-even nuclei with $Z=100-112$ and $N=140-166$, as described in Ref. 45. A rather complex structure of the map is seen. Two maxima of T_{sf} are obtained: one for the known nucleus ^{252}Fm , and the other for the as yet unobserved nucleus $^{270}108$. The maxima are associated with the strong deformed shells at $N=152$ (and a weaker one at $Z=100$) and at $N=162$ and $Z=108$, respectively, appear-

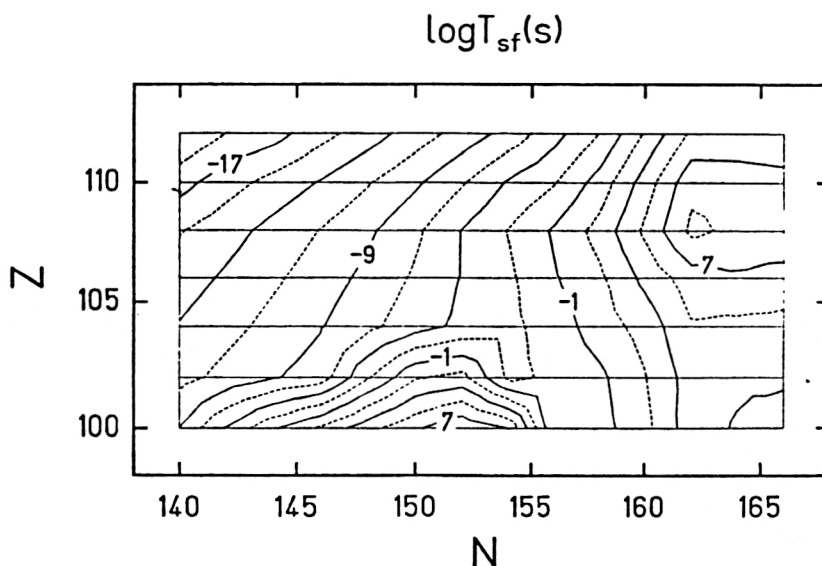


FIG. 8. Contour map of the logarithm of spontaneous-fission half-life T_{sf} , given in seconds.⁴⁵

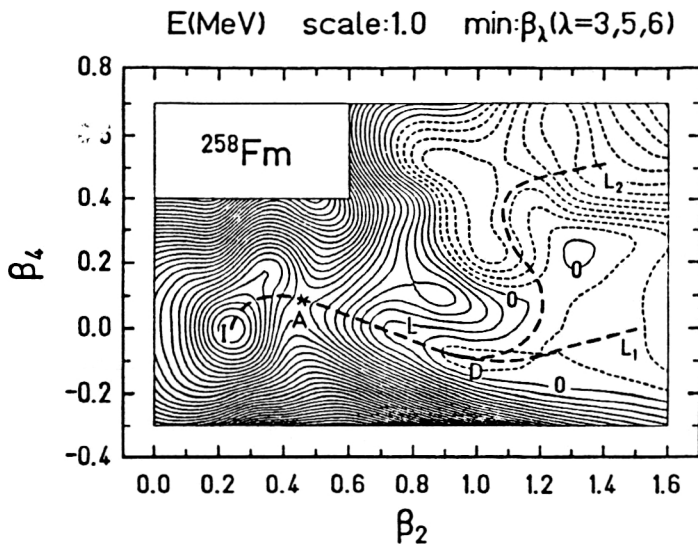


FIG. 9. Contour map of the potential energy E calculated for ^{258}Fm . The numbers at the contour lines give the values of the energy, which is normalized to zero at the equilibrium point I. Solid contour lines correspond to positive energies, and dashed lines to negative energies.²³

ing for the ground-state configuration of these nuclei. The shells result in relatively high fission barriers for these nuclei. The shells at $Z=108$ and $N=162$, obtained in the calculations, are especially strong, qualifying the nucleus $^{270}108$ as a good candidate for a doubly magic deformed nucleus.

6.5. Bimodal fission

In this subsection, we illustrate results related to bimodal fission of ^{258}Fm , i.e., of one of the nuclei for which this process has been observed.

Figure 9 shows a map²³ of the potential energy of ^{258}Fm calculated as a function of the deformations β_2 and β_4 . At each point (β_2, β_4) , the energy is minimized in the β_3, β_5 , and β_6 degrees of freedom. Thus, the analysis is

performed in the 5-dimensional deformation space. A line L close to the static fission trajectory is indicated. It starts at the first minimum (the equilibrium point), passes through the saddle point A, and reaches a shallow second minimum. Then it splits (at the point D) into two trajectories: L_1 and L_2 . One trajectory (L_1) goes into the valley which (as will be shown in Fig. 10) corresponds to more compact shapes (CS) of the nucleus, and the other (L_2) goes into the valley which corresponds to more elongated shapes (ES). One can see that the two fission modes proceeding along the trajectories L_1 and L_2 have the same fission barrier, as not barrier appears beyond the bifurcation point D. Thus, the two modes have the same half-life.

Figure 10 shows the shapes²³ of ^{258}Fm corresponding to the potential energy given in Fig. 9. One can see that the

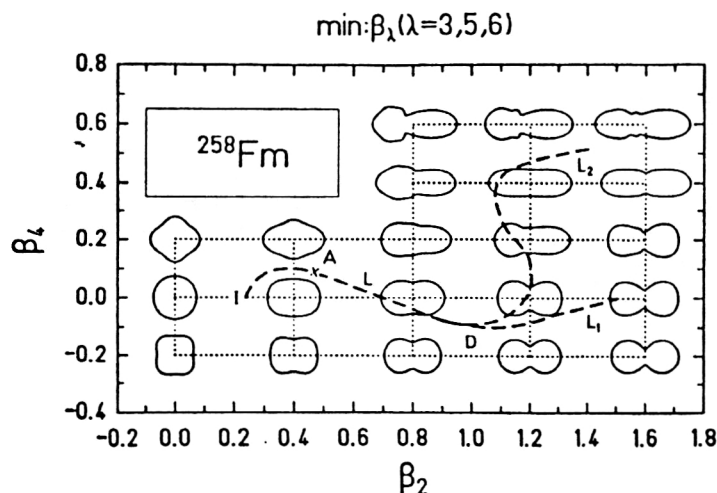
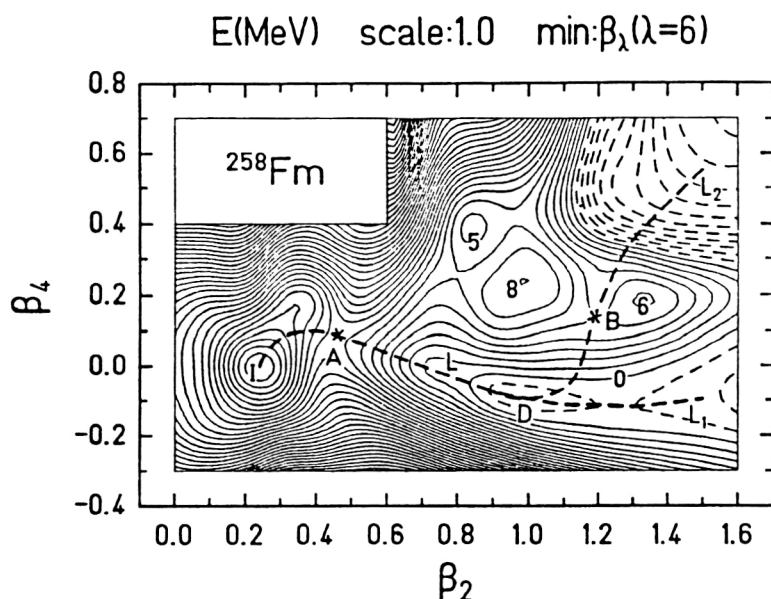


FIG. 10. Shapes of the nucleus ^{258}Fm corresponding to the energies given in Fig. 9 (Ref. 23).



shapes corresponding to the trajectory L_1 are much more compact than those corresponding to L_2 , and they are reflection-symmetric. Both results are in line with experiment.^{5,16–18}

One should stress the important role of the reflection-asymmetric shapes in the analysis of fission of ^{258}Fm , although the observed mass distribution of its fragments is symmetric. Figure 11 shows the potential energy calculated for this nucleus when only symmetric shapes, $\lambda=2, 4, 6$, are considered.²³ One can see that the two fission valleys are separated in this case by a high ridge. Due to this, fission would proceed in such a case only to the

compact-shape valley, since to reach the other valley the nucleus would have to overcome a high (of about 4 MeV) additional barrier. Thus, the bimodal fission would not appear. Only the inclusion of the odd-multipolarity deformations ($\lambda=3, 5$) removes this additional barrier, as seen in Fig. 9.

7. MAGIC DEFORMED NUCLEI

A large shell correction to the energies of nuclei around the nucleus $^{270}108$, seen in Fig. 5, indicates the formation of large shells in the single-particle energy spec-

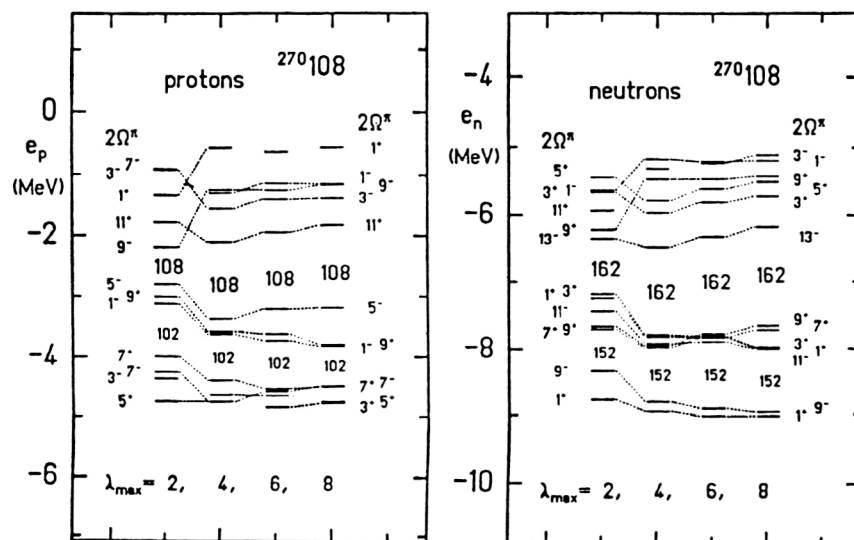


FIG. 12. Proton and neutron spectra of the nucleus $^{270}_{108}$ as functions of the maximal multipolarity λ_{\max} of deformations allowed in it.⁴⁶

tra of these deformed nuclei. It is interesting then to see explicitly these spectra and also the effect on them of the dimension of the deformation space which is used to obtain them.

Figure 12 shows the dependence of the single-particle spectra of the nucleus $^{270}\text{108}$ on the maximal multipolarity λ_{max} of deformations allowed in the nucleus.⁴⁶ At each energy level, the projection of the spin (multiplied by two) of the nucleus on the symmetry axis, 2Ω , as well as the parity, π , are indicated. One can see that a rather small gap at $Z=108$, in the proton spectrum, and a larger gap at $N=162$, in the neutron spectrum, are created by the quadrupole deformation $\lambda=2$. Both gaps are significantly increased, however, by the inclusion of the hexadecapole deformation $\lambda=4$: the gap at $Z=108$ is increased to about 1.2 MeV; and that at $N=162$, to about 1.3 MeV. The inclusion of $\lambda=6$ practically does not change the gap at $Z=108$, but it still increases the neutron gap to about 1.4 MeV. The addition of $\lambda=8$ increases the proton gap to about 1.4 MeV, but it does not change the neutron gap. The further inclusion of $\lambda=10$ leaves the spectra practically unchanged.

Thus, large shells in both the proton and neutron spectra, similar to those observed in magic spherical nuclei, are obtained for the well deformed nucleus $^{270}\text{108}$. To get them, however, one needs to give the nucleus enough freedom to choose the deformation which is really best for it. The nucleus $^{270}\text{108}$, not yet observed in experiments, may be expected then to be a doubly magic deformed nucleus.

8. CONCLUSIONS

The following conclusions may be drawn from the analysis of the properties of the heaviest nuclei performed in recent years (and only partly illustrated in the present short review):

(1) Shell effects play a very important role in the properties of the heaviest nuclei. They decrease the masses of already known nuclei by up to about 5 MeV and the alpha-decay energies by up to about 0.9 MeV. The effects increase the alpha-decay half-lives of these nuclei by up to about 5 orders of magnitude and the spontaneous-fission half-lives by up to about 15 orders of magnitude. Without these effects, some of the heaviest nuclei already observed (like $^{260}\text{106}$ or $^{264}\text{108}$ with half-lives of the order of milli- or microseconds) would not exist at all.

(2) These large shell effects are obtained for nuclei which are, or are expected to be, well deformed. Such large effects were not expected previously for deformed nuclei, which have less symmetry in their shape than spherical nuclei.

(3) To get such large shell effects for deformed nuclei in theoretical calculations, one needs to leave to a nucleus enough freedom in choosing the shape which is really most comfortable for it. In other words, one needs to analyze the properties of a nucleus in a sufficiently large deformation space.

(4) After the experimentally known deformed shell at the neutron number $N=152$, the next deformed shell at $N=162$ is predicted by theoretical calculations. A proton

deformed shell at $Z=108$ is also expected. As both shells are rather strong, the nucleus $^{270}\text{108}$ may be considered as a candidate for a doubly magic deformed nucleus.

(5) One of the consequences of large shell effects in deformed nuclei (which increase their stability) is the expectation that the spherical superheavy nuclei around the predicted doubly magic nucleus $^{298}\text{114}$ do not form an island, separated from the peninsula of known nuclides by a region of unstable deformed nuclei. Instead, they are expected to form a part of the extended peninsula of relatively long-lived nuclides.

(6) Bimodal fission, discovered in recent years, may be described theoretically in a rather natural way if a sufficiently large deformation space is used for this description.

¹ P. Armbruster, *Ann. Rev. Nucl. Part. Sci.* **35**, 135 (1985).

² Yu. Ts. Oganessian and Yu. A. Lazarev, in *Treatise on Heavy-Ion Science*, Vol. 4, edited by D. A. Bromley (Plenum Press, New York, 1985), p. 3.

³ G. Müntzberg, *Rep. Prog. Phys.* **51**, 57 (1988).

⁴ D. C. Hoffman and L. P. Somerville, in *Particle Emission from Nuclei*, Vol. 3, edited by D. N. Poenaru and M. S. Ivascu (CRC Press, Boca Raton, 1989), p. 1.

⁵ E. K. Hulet, J. F. Wild, R. J. Dougan *et al.*, *Phys. Rev. C* **40**, 770 (1989).

⁶ G. T. Seaborg and W. D. Loveland, *The Elements Beyond Uranium* (Wiley, New York, 1990).

⁷ S. Hofmann, in *Proc. of the 24th Zakopane School on Physics*, Vol. 1, edited by J. Styczen and Z. Stachura (World Scientific, Singapore, 1990), p. 199.

⁸ A. Sobczewski, F. A. Gareev, and B. N. Kalinkin, *Phys. Lett.* **22**, 500 (1966).

⁹ H. Meldner, *Ark. Fys.* **36**, 593 (1967).

¹⁰ Z. Patyk, A. Sobczewski, P. Armbruster, and K. -H. Schmidt, *Nucl. Phys.* **A491**, 267 (1989).

¹¹ H. J. Krappe, J. R. Nix, and A. J. Sierk, *Phys. Rev. C* **20**, 992 (1979).

¹² J. Randrup, C. F. Tsang, P. Moller *et al.*, *Nucl. Phys.* **A217**, 221 (1973).

¹³ J. Randrup, S. E. Larsson, P. Moller *et al.*, *Phys. Rev. C* **13**, 229 (1976).

¹⁴ A. Sobczewski, *Fiz. Elem. Chastits At. Yadra* **10**, 1170 (1979) [*Sov. J. Part. Nucl.* **10**, 466 (1979)].

¹⁵ W. D. Myers and W. J. Swiatecki, *Ark. Fys.* **36**, 343 (1967).

¹⁶ D. C. Hoffman, *Acc. Chem. Res.* **17**, 235 (1984).

¹⁷ E. K. Hulet, J. F. Wild, R. J. Dougan *et al.*, *Phys. Rev. Lett.* **56**, 313 (1986).

¹⁸ E. K. Hulet, in *Proc. of the 5th Intern. Conf. on Nuclei Far from Stability*, Rosseau Lake, 1987, edited by I. S. Towner (AIP Conf. Proc. **164**, New York, 1988), p. 810.

¹⁹ U. Brosa, S. Grossmann, and A. Müller, *Z. Phys. A* **325**, 241 (1986).

²⁰ K. Depta, J. A. Maruhn, W. Greiner *et al.*, *Mod. Phys. Lett.* **A1**, 377 (1986).

²¹ P. Möller, J. R. Nix, and W. J. Swiatecki, *Nucl. Phys.* **A469**, 1 (1987); **A492**, 349 (1989).

²² V. V. Pashkevich, *Nucl. Phys.* **A477**, 1 (1988).

²³ S. Cwiok, P. Rozmej, A. Sobczewski, and Z. Patyk, *Nucl. Phys.* **A491**, 281 (1989).

²⁴ V. M. Strutinsky, *Nucl. Phys.* **A95**, 420 (1967); **A122**, 1 (1968).

²⁵ S. G. Nilsson, C. F. Tsang, A. Sobczewski *et al.*, *Nucl. Phys.* **A131**, 1 (1969).

²⁶ S. Cwiok, J. Dudek, W. Nazarewicz *et al.*, *Comput. Phys. Commun.* **46**, 379 (1987).

²⁷ M. Bolsterli, E. O. Fiset, and J. R. Nix, in *Proc. of the 2nd IAEA Symposium on Physics and Chemistry of Fission* (IAEA, Vienna, 1969), p. 183.

²⁸ V. G. Soloviev, *Theory of Complex Nuclei* (Pergamon Press, Oxford, 1976) [Russ. original, Nauka, Moscow, 1971].

²⁹ A. Sobczewski, Z. Szymanski, S. Wycech *et al.*, *Nucl. Phys.* **A131**, 67 (1969).

- ³⁰M. Brack, J. Damgaard, A. S. Jensen *et al.*, *Rev. Mod. Phys.* **44**, 320 (1972).
- ³¹H. C. Pauli, *Phys. Rep.* **7C**, 35 (1973); *Nukleonika* **20**, 601 (1975).
- ³²K. Pomorski, T. Kaniowska, A. Sobiczewski, and S. G. Rohozinski, *Nucl. Phys.* **A283**, 394 (1977).
- ³³V. V. Pashkevich, *Nucl. Phys.* **A133**, 400 (1969).
- ³⁴S. E. Larsson, *Phys. Scr.* **8**, 17 (1973).
- ³⁵S. G. Rohozinski and A. Sobiczewski, *Acta. Phys. Pol.* **B12**, 1001 (1981).
- ³⁶S. Cwiok, V. V. Pashkevich, J. Dudek, and W. Nazarewicz, *Nucl. Phys.* **A410**, 254 (1983).
- ³⁷K. Böning, Z. Patyk, A. Sobiczewski, and G. Cwiok, *Z. Phys. A* **325**, 479 (1986).
- ³⁸S. Cwiok and A. Sobiczewski, *Z. Phys. A* **342**, 203 (1992).
- ³⁹V. E. Viola, Jr. and G. T. Seaborg, *J. Inorg. Nucl. Chem.* **28**, 741 (1966).
- ⁴⁰D. N. Poenaru and M. Ivascu, *J. Phys.* **44**, 791 (1983).
- ⁴¹Y. Hatsukawa, H. Nakahara, and D. C. Hoffman, *Phys. Rev. C* **42**, 674 (1990).
- ⁴²B. Buck, A. C. Merchant, and S. M. Perez, *J. Phys. G* **17**, 1223 (1991).
- ⁴³A. Sobiczewski, Z. Patyk, and S. Cwiok, *Phys. Lett.* **224B**, 1 (1989).
- ⁴⁴A. Baran, K. Pomorski, A. Lukasiak, and A. Sobiczewski, *Nucl. Phys.* **A361**, 83 (1981).
- ⁴⁵Z. Patyk, J. Skalski, A. Sobiczewski, and S. Cwiok, *Nucl. Phys.* **A502**, 591c (1989).
- ⁴⁶Z. Patyk and A. Sobiczewski, *Nucl. Phys.* **A533**, 132 (1991).

This article was published in English in the original Russian journal. It is reproduced here with the stylistic changes by the Translation Editor.